ResearchGate

See discussions, stats, and author profiles for this publication at: https://www.researchgate.net/publication/231627816

Disorder in Binary Polymer Systems near Their Critical Region Studied by Low-Frequency Raman Spectroscopy

ARTICLE *in* THE JOURNAL OF PHYSICAL CHEMISTRY B · MARCH 2001

Impact Factor: 3.3 · DOI: 10.1021/jp0016941

CITATIONS
8

READS
29

2 AUTHORS, INCLUDING:

Sviatoslav Kirillov

Joint Department of Electrochemical Energy …

91 PUBLICATIONS **537** CITATIONS

SEE PROFILE

Available from: Sviatoslav Kirillov
Retrieved on: 23 January 2016

ARTICLES

Disorder in Binary Polymer Systems near Their Critical Region Studied by Low-Frequency Raman Spectroscopy

Sviatoslav A. Kirillov*,†,‡ and Tatiana M. Kolomiyets†

Foundation of Research and Technology—Hellas, Institute of Chemical Engineering and High-Temperature Chemical Processes (ICE/HT-FORTH), P.O. Box 1414, 265 00 Patras, Greece

Received: May 4, 2000; In Final Form: November 10, 2000

Low-frequency Raman spectra of a diblock copolymer of polystyrene and polyisoprene (PS−PI) and a polystyrene−polybutadiene blend (PS−PB) have been studied. Low-frequency features, viz., the quasi-elastic lines, Boson peaks, and vibrational lines, if present, have been fitted to known theoretical expressions. It has been found for the first time that, in the diblock, the Boson peaks manifest themselves at frequencies characteristic for homopolymers; that is, big enough regions formed by pure components exist in the diblock. The temperature dependence of the overall integrated intensity in the low-frequency region undergoes a break at the order−disorder transition temperature of the PS−PI diblock and manifests a marked nonlinearity near the temperature of macrophase separation of the PS−PB blend.

I. Introduction

During the past few decades, low-frequency Raman spectra of amorphous solids have attracted much attention of theoreticians and experimentalists.[1−3] It is well-established now that the low-frequency Raman spectrum of an amorphous solid comprises the following contributions: (i) the Rayleigh scattering caused by slow motions of big molecular aggregates, or α-relaxation; (ii) the quasi-elastic (QE) scattering arising due to faster motions of smaller molecular units, or β-relaxation, occurring in the picosecond time domain; (iii) the so-called Boson peak. The latter, most probably, represents acoustic modes of the sample becoming active in Raman scattering due to a breakdown of selection rules in amorphous materials.[4] Since the Rayleigh scattering is practically outside the spectral window in conventional Raman studies, the QE scattering and Boson peaks are the major contributions to the Raman pattern of amorphous solids. These contributions have even been claimed universal properties of any amorphous material, polymers in first place.

Low-frequency Raman spectroscopy is widely employed for studying individual polymers. Such studies are of great help for better understanding polymer dynamics in the vicinity of the glass transition. However, this method has never been used for studies of the structure and dynamics of polymer blends. Meanwhile, it seems to be prospective for the characterization of advanced polymer blends, due to its great sensitivity to disordering in solids.

Mixing incompatible polymers, one can obtain two main types of binary polymer systems with significantly modified properties: two-component blends and the so-called diblock copolymers. In the former, two homopolymers are physically mixed; at a certain temperature these blends can become incompatible and undergo *macrophase* separation. In the latter, two homopolymers, A and B, are chemically joined, forming covalently bonded A and B blocks, and therefore may be considered as single-component systems which cannot macrophase separate. However, due to unfavorable interactions between the blocks, diblock copolymers can undergo *microphase* separation, or the so-called order−disorder transition (ODT). The temperature interval where such structural and dynamic transformations in polymers occur is often referred to as the critical region.

The structure and dynamics of advanced polymer blends at the vicinity of their critical regions are now studied by different high-resolution methods, and the presence and spreading of certain heterogeneities around the ODT have been deduced.[5,6] As an example, we refer to the most recent fascinating proof of the existence of two relaxation times corresponding to the constituent homopolymers in diblocks.[7]

In this paper we use the low-frequency Raman scattering as an instrument of investigation of polymer blends. We report the low-frequency Raman data for a polystyrene−polyisoprene (PS−PI) diblock copolymer and for a polystyrene−polybutadiene (PS−PB) blend near their critical region and demonstrate how these data could be used for characterization purposes.

II. Experimental Section

The PS−PI diblock used in this investigation was the same as that studied in refs 8 and 9 in great detail. Its ODT temperature (359 K) was found by means of the small-angle X-ray scattering technique. As follows from calorimetric measurements, it exhibits two distinct glass-transition temperatures, T_g, at 334 and 211 K corresponding to polystyrene- and polyisoprene-rich phases, respectively. For this reason we assumed the presence of two Boson peaks in the Raman spectra of the diblock.

† Permanent address: Institute for Technological and Information Innovations, P.O. Box 263, 252134 Kyiv-134, Ukraine.
‡ E-mail: kir@i.kiev.ua.

10.1021/jp0016941 CCC: $20.00 © 2001 American Chemical Society
Published on Web 03/29/2001

The PS−PB blend was the same as that studied in ref 10. It was prepared by mixing in solution and underwent macrophase separation at 347 K. The glass-transition temperature of PB (mainly *cis*-1,4) was equal to 180 K. As the samples became opaque below the macrophase separation temperature, our studies of the PS−PB blend were performed at temperatures *above* the macrophase separation temperature, when the substance remained transparent.

PS and PB are well characterized by neutron-scattering and low-frequency Raman data obtained in the broad temperature interval from 6 to 440 K.[11−15] At temperatures well below T_g, from 6 to 35 K, PS demonstrates the pronounced Boson peak of a Lorentzian-like form located at approximately 15−18 cm^{-1} and strongly overlapped by the vibrational line at 50−70 cm^{-1}, which may be assigned as the damped libration of the phenyl ring.[16] The neat Lorentzian-like Boson peak in PB is located at approximately 20−25 cm^{-1} and remains "visible" up to approximately 200 K; the presence of a vibrational line in the low-frequency Raman spectrum of PB is disputable.[13] In PI, the Boson peak is situated at somewhat higher frequencies than in PS and PB, and its profile is intermediate between Lorentzian-like and Gaussian-like; the low-frequency Raman pattern is free of vibrational contributions.[15]

Raman spectra were recorded on a Spex 1403 double monochromator in 90° geometry, in the Stokes region from 4.0 to 150.0 cm^{-1} through each 0.1 cm^{-1}. Both polarized (VV) and depolarized (VH) spectra were obtained. Since the Raman scattering appeared to be totally depolarized, the VH components were used for further analyses. Spectra were subjected to the preliminary background noise correction; the $(\omega_0 - \omega)^{-4}$ dependence of scattering (ω_0 is the frequency of the excitation light and ω is the Raman shift) was also taken into account.

Usually, Boson peaks dominate the Raman spectra at temperatures well below T_g. At ambient temperatures, where the ODT transitions take place, they are hidden under the envelope of the significantly broadened QE line. Therefore, we have studied the bare Boson peaks in the PS−PI diblock at 77 K.

To analyze the spectra obtained in more detail and to operate with the parameters of each component of the overall low-frequency Raman spectrum separately, we have employed one of the standard interpretation schemes based on the so-called superposition approach. The relevant theoretical background is described in the next section.

III. Theoretical Background

It has become evident from the current literature that two main approaches to the low-frequency Raman data fits exist, where the QE and Boson peak features are represented either as a convolution or as a superposition. A detailed analysis of the advantages and shortcomings of both approaches was performed recently in ref 17.

The convolution approach (see, e.g., refs 17 and 18) relies on ideas originated from the "indirect" scattering mechanism of Winterling.[19] It is assumed that the QE line represents a low-frequency relaxation-like part of the one-phonon response function. In other words, the vibrational excitations are coupled to some relaxing variable that induces broadening to each frequency of the Boson peak. Such coupling leads to the conclusion that the overall low-frequency Raman spectrum of an amorphous material is represented by a convolution of the vibrational (Boson peak) and relaxational contributions, the latter being characterized by a simple exponential relaxation function.

The convolution approach is quite common in studies of neat polymers. However, it appears to be inappropriate for polymer blends. By construction, it needs the detailed knowledge of the position and profile of the Boson peak at the lowest possible temperatures, when the QE contribution is negligibly small. In what follows we will show that, in blends, the Boson peak positions are shifted if compared with pure homopolymers.

In the superposition approach, the spectrum is modeled as the sum of two separate contributions: a Lorentzian line describes the QE part, and a generalization of the Martin−Brenig model[20] is used for the Boson peak. Possible low-lying vibrational lines may also be taken into account if they seriously affect the Boson peak shape.

According to Martin and Brenig,[20] the lack of periodicity in an amorphous solid and the subsequent electrical and mechanical disorder generate spatial fluctuations in the elastic and photon−phonon coupling constants. These assumptions lead to the following expression of the Boson peak:

$$I_{\mathrm{Boson}}(\omega) \propto \frac{I_{\mathrm{expt}}(\omega)}{\omega[n(\omega)+1]}\omega^2\left[g_{\mathrm{TA}}(\omega)E_{\mathrm{TA}} + \frac{2}{3}g_{\mathrm{LA}}(\omega)E_{\mathrm{LA}}\right] \quad (1)$$

where the VH contribution to overall scattering at 90° geometry is postulated. The fractional factor on the right-hand side of eq 1 arises due to averaging procedures. The expression in the square brackets in the denominator is the Bose factor for the Stokes Raman, $n(\omega) = [\exp(\hbar\omega/k_{\mathrm{B}}T) - 1]^{-1}$, where $\hbar$ and k_{B} are Planck's and Boltzmann's constants, respectively. The E values with respective indices are specific combinations of the photon−phonon coupling coefficients, and $g_i(\omega)$ are the space Fourier transforms of $G_{\mathrm{dis}}(r)$, the correlation function of the disorder in the amorphous solid.

Using a Gaussian $G_{\mathrm{dis}}(r)$, Martin and Brenig have arrived at the Boson peak of an asymmetric quasi-Gaussian profile. However, it has been proven inadequate to fit a body of experimental data for various substances.[21] The use of an exponential $G_{\mathrm{dis}}(r)$[21] changes the profile of the Boson peak from Gaussian-like to Lorentzian-like, which seems to conform better with the measured spectra.

Even better agreement and flexibility are provided by a generalization proposed in refs 15 and 22. It accounts for a manifold of spectral shapes ranging from the quasi-Gaussian to the quasi-Lorentzian limit. Writing the space correlation function as $G_{\mathrm{dis}}(r) = \exp\{-[(r^2 + R_1^2)^{1/2} - R_1]/R_2\}$, where r is the distance, R_2 is the structure correlation radius, and R_1 is a measure of the steepness of $G_{\mathrm{dis}}(r)$, one obtains

$$g_{\mathrm{TA}}(\omega) = 4\pi c\frac{\Omega_{2,\mathrm{TA}}}{\Omega_{1,\mathrm{TA}}}\exp\left(\frac{\Omega_{2,\mathrm{TA}}}{\Omega_{1,\mathrm{TA}}}\right)\frac{K_2[z_{\mathrm{TA}}(\omega)]}{z_{\mathrm{TA}}{}^2(\omega)} \quad (2a)$$

$$g_{\mathrm{LA}}(\omega) = \left(\frac{v_{\mathrm{TA}}}{v_{\mathrm{LA}}}\right)^5 4\pi c\frac{\Omega_{2,\mathrm{LA}}}{\Omega_{1,\mathrm{LA}}}\exp\left(\frac{\Omega_{2,\mathrm{LA}}}{\Omega_{1,\mathrm{LA}}}\right)\frac{K_2[z_{\mathrm{LA}}(\omega)]}{z_{\mathrm{LA}}{}^2(\omega)} \quad (2b)$$

where $K_2(x)$ is the modified Bessel function of the second kind, $\Omega_{i,j} = v_j/R_i$, v_j is the respective sound velocity, and $z_j(\omega) = (\omega^2 + \Omega_{2,j}{}^2)^{1/2}/\Omega_{1,j}$.

The Ω_2 value is close to the peak position of the Boson peak, and the Ω_2/Ω_1 value serves as a measure of the type of its profile. It tends to be Lorentzian-like at $\Omega_2/\Omega_1 \leq 0.1$ and Gaussian-like at $\Omega_2/\Omega_1 \geq 50$.

The QE scattering is most often considered in terms of the model proposed by Theodorakopoulos and Jäckle.[23] It attributes the QE scattering to the population interplay between two energetically equal defect states described by different polarizabilities and represented by a symmetric double-well potential. The following expression for the Raman intensity holds:

$$I_{QE}(\omega) = \frac{I_{expt}(\omega)}{\omega[n(\omega)+1]}\int_0^\infty \frac{\tau(V)}{1+\omega^2\tau^2(V)}P(V)\,dV \approx \frac{I_{expt}(\omega)}{\omega[n(\omega)+1]}\frac{\tau}{1+\omega^2\tau^2} \quad (3)$$

where the fractional factor is of the same nature as in eq 1. $P(V)$ is the distribution of activation energies (barriers separating adjacent wells) V, and the relaxation time τ (time scale for well-to-well hopping) follows an Arrhenius temperature dependence, $\tau(V) = \tau_0 \exp(V/k_BT)$. It is customary to use the second equality in eq 3, which in fact presumes that all the V values are equal and then $1/\tau$ designates the half-width at half-height (HWHH) of the QE line.

The profile of the low-lying vibrational line of PS has been modeled as described in ref 24. The method employed enables one to fit real line profiles intermediate between Gaussian and Lorentzian by an analytical function (an analogue of the Voigt function) which has an analytical counterpart in the time domain. It is based on the model time-correlation function written in the form

$$G_\nu(t) = \exp\{-[(t^2 - {\tau_1}^2)^{1/2} - \tau_1]/\tau_2\} \quad (4)$$

where τ_1 is close to the vibrational frequency modulation time τ_ω and τ_2 to the dephasing time τ_ν. These characteristic times are widely used in the studies of the dynamics of liquids; for the latest review, see refs 25 and 26.

The Fourier transform of eq 4 can be performed analytically, giving the vibrational line profile as

$$I(V) = 2nc\exp(\tau_1/\tau_2)({\tau_1}^2/\tau_2)K_1(x)/x \quad (5)$$

where $K_1(x)$ is the modified Bessel function of the second kind, ν_0 is the peak wavenumber, $n = 2$ if $\nu_0 = 0$ and $n = 1$ if $\nu_0 \neq 0$, and $x = \tau_1[4\pi^2c^2(\nu - \nu_0)^2 + 1/{\tau_2}^2]^{1/2}$.

Equations 1−5 are used in our computation procedure. This version of the superposition approach has been successfully employed in our recent studies of polymers,[14,15] viscous[14,15] and hydrogen-bonded[27] liquids, and ionic glass-formers.[17]

IV. Results and Discussion

A. Neat Polymers. The low-frequency Raman spectra of PS and PI have been well described in refs 11−15, and results of their fits are analyzed in detail in our recent papers, where the parameters of the QE line, Boson peak, and low-lying vibrational modes are given.[14,15] Therefore, we will briefly discuss only the spectrum of neat polybutadiene, where the presence of a vibrational line is suspected. Such a conclusion has been made in the course of the analysis of Raman data replotted in the susceptibility format,[13] $\chi(\omega) = I_{expt}(\omega)/[n(\omega)+1]$, where χ means the susceptibility, and other values have been defined previously.

In Figure 1 a depolarized spectrum of PB along with the fitting data is shown in the intensity and susceptibility formats, as well as in double logarithmic coordinates, representations widely used in spectroscopic practice.[11−13] This spectrum is practically identical to that published in ref 13. It is well seen from our fitting data that an apparent flat maximum on the susceptibility plot located at approximately 30 cm^{-1} has nothing to do with vibrational contributions. It is rather the result of an interplay between the QE contribution and the Boson peak. The maxima of these features on the susceptibility plot are shifted as compared to the raw spectral data. Analysis shows that the

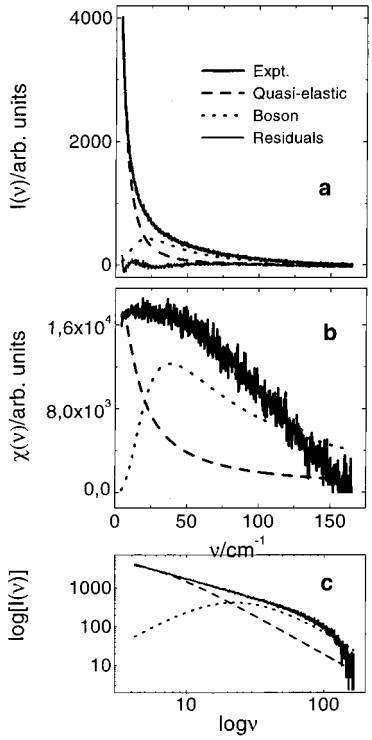

Figure 1. Low-frequency Raman spectrum of polybutadiene at 347 K and its components (a), and the same spectrum replotted in susceptibility (b) and bilogarithmic (c) coordinates to ensure the comparison with refs 11 and 13.

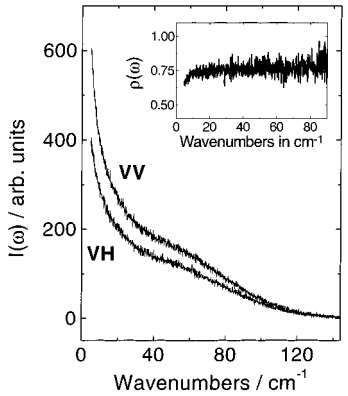

Figure 2. VV and VH low-frequency Raman spectra of the PS−PI diblock at 368 K. The depolarization ratio $\rho(\omega) = I_{VH}(\omega)/I_{VV}(\omega)$ is shown in the inset.

respective maxima of the susceptibility spectrum can be expressed as $\omega^x_{QE} = \Omega_{QE}$ and $\omega^x_{Boson} \approx n\Omega_1$, where $n = \sqrt{1.5}$ if the space correlation function in a medium is Gaussian and $n = \sqrt{3}$ if the space correlation function in a medium is exponential.

The parameters of QE lines, Boson peaks, and vibrational lines obtained in our fits are discussed later, along with the respective parameters of the blends. Mistakes in frequencies determined in these fits do not exceed 1 cm^{-1}, and relative mistakes in integrated intensities are less than 10%.

B. PS−PI Diblock: Two Boson Peaks. Representative spectra of the PS−PI diblock registered at the vicinity of the ODT temperature are plotted in Figure 2. The depolarization ratio $\rho = I_{VH}(\nu)/I_{VV}(\nu)$ is equal to 0.75 and remains constant within the whole spectral interval studied. Therefore, in further analyses we operate with the VH Raman spectra.

As expected, the spectra are strongly influenced by the significantly broadened QE line. At low temperatures, the

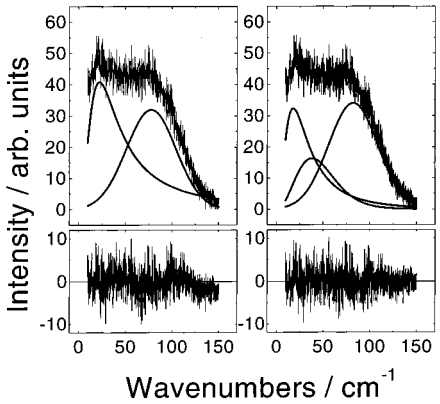

Figure 3. Low-frequency Raman spectrum of the PS−PI diblock at 77 K and results of its modeling (top) and differences between the experimental spectrum and data fits (bottom). Left: one Boson peak, weighted root-mean-square error 2.92. Right: two Boson peaks, $\Omega_2/\Omega_1 < 0.1$ (PS), $\Omega_2/\Omega_1 \approx 0.39$ (PI), weighted root-mean-square error 2.72.

contribution of the QE line to the overall spectrum becomes negligible. Therefore, to study the Boson peak region in greater detail, we have made low-temperature measurements.

The low-frequency VH Raman spectrum of the PS−PI diblock at 77 K is shown in Figure 3. Our computations prove that the assumption concerning the presence of two Boson peaks in the diblock better agrees with experimental data. The lower-frequency Boson peak profile (PS) is Lorentzian-like ($\Omega_2/\Omega_1 < 0.1$), and the higher-frequency Boson peak profile (PI) is intermediate between Lorentzian-like and Gaussian-like ($\Omega_2/\Omega_1 \approx 0.39$), as in pure homopolymers.[14,15] Attempts to fit the data to the one Boson peak fail. The first, most direct, evidence is the general appearance of residuals presented in the bottom part of Figure 3. It is well seen with the naked eye that the dispersion of residuals is much less in the case of the two-peak fit. Respective root-mean-square errors prove this finding: these are equal to 2.92 for the best one-peak fit and to 2.72 for the best two-peak fit.

In refs 5 and 6, distinct evidence of the existence of two different local environments (strong composition fluctuations) has been demonstrated for diblocks even far above the ODT. Indeed, such different environments in the PS−PI diblock are clearly seen in the low-frequency Raman experiment. Two Boson peaks with parameters characteristic of pure components reflect the presence of quite big regions formed by homopolymers in the blend. Acoustic vibrations of polymer chains of one kind are not significantly perturbed by the presence of the "impurity" chains of another kind, and the acoustic phonons are propagating almost like those in pure homopolymers.

C. Temperature Dependencies: Frequencies. The low-temperature data obtained for the PS−PI diblock serve as a basis for subsequent data fits, where the presence of two distinct Boson peaks has been postulated. The same approximation is certainly valid for the PS−PB blend consisting of the mechanical mixture of two immiscible components. It should be remembered that, for the PS−PB blend, we are able to study only the temperature region above the macrophase separation temperature. Below this temperature, the sample becomes opaque and the signal-to-noise ratio significantly drops.

Boson peak frequencies obtained in these fits are plotted in Figure 4. The temperature dependencies of frequencies in the PS−PI diblock show a barely visible break at T_{ODT}, being practically linear below and above this temperature. The same tendency persists in the high-temperature phase of the PS−PB

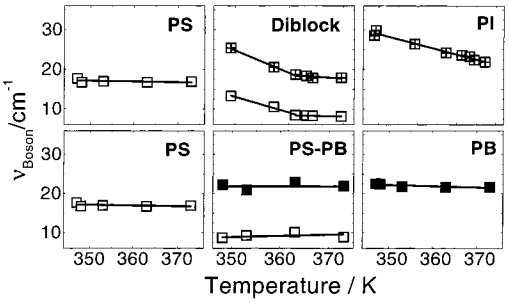

Figure 4. Temperature dependencies of the Boson peak frequencies in the low-frequency Raman spectra of the PS−PI diblock and the PS−PB blend and corresponding neat homopolymers.

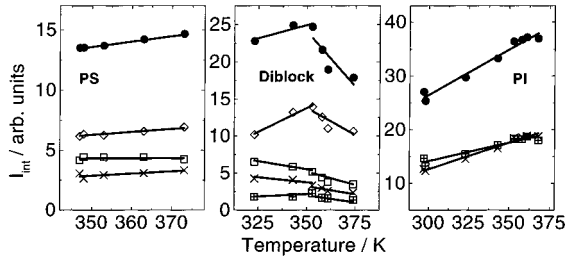

Figure 5. Temperature dependencies of integrated intensities in the low-frequency Raman spectra of polystyrene, polyisoprene, and the PS−PI diblock. Key: full circles, overall spectra; times signs, overall quasi-elastic lines; squares, Boson peaks; tilted squares, vibrational line.

blend. The data clearly demonstrate that, in polymer blends, the Boson peak frequencies are lower than in constituting homopolymers.

We have tried to interpret this fact on the basis of the definition of the Boson peak frequency in an amorphous solid, $\Omega_{i,j} = v_j/R_i$, where v_j is the respective sound velocity and R_i is the structure correlation radius. To estimate the R_i value, the sound velocity data are required. Such data for polymer blends are scarce; for the PS−PI diblock and PS−PB blend these are unknown. Theory[26] predicts that the sound velocity in the blend is a weight average of the corresponding values in the pure components. This means that, to explain the data obtained, we have to suppose that the correlation radii (micro-ordered domains) in blends are greater than in constituting homopolymers. Such a conclusion contradicts common sense.

On the other hand, the theory by Brodsky et al.[29] anticipates that, in the spectra of solid solutions, transversal vibrations of both components are shifted to lower frequencies if compared to those of pure substances. This explanation better corresponds to the results obtained since the Boson peak positions are determined mainly by the $\Omega_{1,TA}$ values. However, the theory by Brodsky et al. deals with a homogeneous ionic solid solution, the order of magnitude of a typical ionic radius being about several angstroms, whereas in polymer blends, domain sizes are several tens or even hundreds of angstroms. Such a fact makes the application of this theory to polymers questionable, and much more work is to be undertaken to better understand the nature of this intriguing feature.

D. Temperature Dependencies: Intensities. Another noticeable conclusion follows from our intensity measurements. Temperature dependencies of the integrated intensities of the low-frequency Raman spectra are plotted in Figures 5 and 6 along with the data for homopolymers. In PS and PI these temperature dependencies are linear. In the PS−PI diblock, Figure 5, they are linear either in ordered or in disordered phases, and undergo a break at the ODT. Below T_{ODT}, in the ordered phase, they increase on heating, like in homopolymers. Above

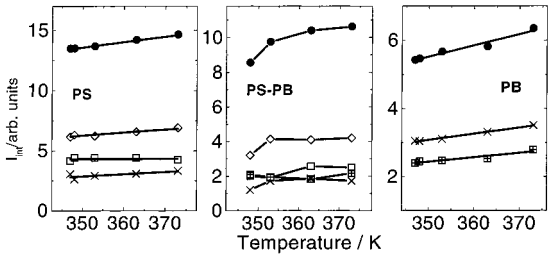

Figure 6. Temperature dependencies of integrated intensities in the low-frequency Raman spectra of polystyrene, polybutadiene, and the PS−PB blend. For notation see Figure 5.

T_{ODT}, in the disordered phase, they decrease on heating. Naturally, such a result is model-independent and is not affected by the underlying assumption concerning two Boson peaks in the diblock. However, the fitting data reveal the same trend in the temperature dependencies of all partial intensities.

In the PS−PB blend, Figure 6, a marked nonlinearity is found for integrated intensities, as distinct from homopolymers. Fitting data (partial intensities) tell the same story.

We conceive the data presented in Figures 5 and 6 as being highly promising for the future use of the low-frequency Raman technique in the characterization of polymer blends. Breaks and nonlinearities of *all* partial intensities ensure that these spectroscopic features are strongly influenced by interchain interactions occurring in the bulk polymer mixture.

Raman intensities in polymers may be interpreted in terms of Stephen's model of the low-frequency Raman scattering,[30] which employs the density fluctuations concept. In this model, the Raman intensity can be written as

$$I(\omega) = \frac{\alpha^2\omega^4}{2\pi c^4}(\mathbf{E}_0\cdot\mathbf{E}_s)^2 S(\mathbf{Q},\omega) \qquad (6)$$

where α is the polarizability of a scatterer, $\mathbf{E}_0$ and $\mathbf{E}_s$ are the unit vectors in the directions of the incident and scattered radiations, respectively, $\mathbf{Q}$ is the wave vector, and the value $S(\mathbf{Q},\omega)$ determines the so-called structure factor of the system studied as $S(\mathbf{Q}) \propto \int d\omega\ S(\mathbf{Q},\omega)$.

Structure factors play a fundamental role in the thermodynamics of polymer blends. Several generally accepted theories exist,[31,32] enabling one to predict the ODT temperature in terms of the structure factor, concentrations, and some structure parameters. These theories serve as a basis for experimental measurements of the ODT temperature, since it is known from X-ray and neutron scattering in solids[33] that the peak occurring on the dependence of the scattered intensity on $\mathbf{Q}$ is determined by the same structure factor, $I \propto S(\mathbf{Q})$. That is, one can expect that the temperature dependencies of the Raman and, say, the small-angle X-ray scattering (SAXS) intensities should be similar. This is true for the PS−PI diblock; Raman intensities show a break near the critical temperature (Figure 7). Moreover, Raman data seem to be even more sensitive to the ODT than SAXS.[8] The temperature dependence of SAXS intensities[8] for the PS−PI diblock demonstrates two maxima, and to correctly determine the critical temperature, one has to analyze the temperature dependence of SAXS line widths.[8]

Conclusions

In this paper we deal with the low-frequency Raman spectra of the block copolymer of PS and PI and the blend of PS and PB. It is found that, in the diblock, the Boson peaks manifest themselves at frequencies characteristic of pure polymers, so that large enough regions formed by pure components exist in the diblock. This conclusion is in line with ideas concerning different local environments or, in other words, concentration fluctuations in block copolymers.[5,6]

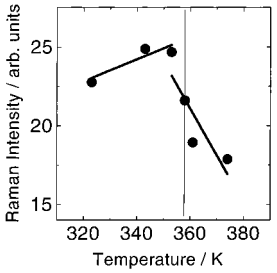

Figure 7. Intensities in the low-frequency Raman spectra of the PS−PI diblock. Straight lines are guides for the eye; the ODT temperature found by SAXS[8] (359 K) is indicated by a line.

The temperature dependence of the integrated intensity of the low-frequency Raman spectra undergoes a break at T_{ODT} in the PS−PI diblock and reveals a marked nonlinearity in the vicinity of the macrophase separation temperature in the PS−PB blend. It is found that the temperature dependencies of the Raman intensities are even sharper than the temperature dependencies of SAXS[8] widely used for characterization purposes. This observation could be employed for the characterization of advanced polymer blends near their critical temperatures.

Acknowledgment. We are indebted to S. H. Anastasiadis, G. Floudas, G. Fytas, N. Hadjichristidis, and D. Vlassopoulos (Institute of Electronic Structure and Laser-FORTH, Heraklion, Crete, Greece) for providing us with samples and to G. Voyiatzis (ICE/HT-FORTH) for Raman measurements. Numerous fruitful discussions with them and G. Papatheodorou (ICE/HT-FORTH) are gratefully acknowledged. Thanks are due to the NATO Scientific Affairs Division for financial support within the framework of the Science for Stability program, GR-POLY-BLEND-SfS Project, Outreach dimension.

References and Notes

(1) *Glasses and Amorphous Materials: Frontiers in Material Science*; Special Issue of *Science* **1995**, *267*, 1924.
(2) *Spectroscopic Studies of Glasses and Sol−Gel Materials*; Corset, J., Ed.; Special Issue of *J. Raman Spectrosc.* **1996**, *27*, 705.
(3) *Relaxation in Glass-Forming Liquids*; Barnes, A. J., Vij, J. K., Eds.; a collection of invited papers in honor of Prof. G. P. Johari; *J. Mol. Struct.* **1999**, *479*, 111.
(4) Shuker R.; Gammon, R. W. *Phys. Rev. Lett.* **1976**, *25*, 222.
(5) Fytas, G.; Anastasiadis S. H. In *Disorder Effects on Relaxation Processes*; Richert, R., Blumen, A., Eds.; Springer: Berlin, 1994; p 697.
(6) Kumar, S. K.; Colby, R. H.; Anastasiadis, S. H.; Fytas, G. *J. Chem. Phys.* **1996**, *105*, 3777.
(7) Floudas, G.; Fytas, G.; Reisinger, T.; Wegner, G. *J. Chem. Phys.* **1999**, *111*, 9129.
(8) Floudas, G.; Pakula, T.; Fischer, E. W.; Hadjichristidis, N.; Pispas, S. *Acta Polym.* **1994**, *45*, 176.
(9) Floudas, G.; Fytas, G.; Hadjichristidis, N.; Pitsikalis, M. *Macromolecules* **1995**, *28*, 2369.
(10) Fytas, G.; Vlassopoulos, D.; Meier, G.; Likhtman, A.; Semenov, A. N. *Phys. Rev. Lett.* **1996**, *76*, 3586.
(11) Sokolov, A. P.; Buchenau, U.; Steffen, W.; Frick, B.; Wischnewski, A. *Phys. Rev. B* **1995**, *52*, R9815.
(12) Novikov, V. N.; Sokolov, A. P.; Strube, B.; Surovtsev, N. V.; Duval, R.; Mermet, A. *J. Chem. Phys.* **1997**, *107*, 1057.
(13) Sokolov, A. P.; Novikov, V. N.; Strube, B. *Phys. Rev. B* **1997**, *56*, 5042.
(14) Kirillov, S. A.; Perova, T. S.; Faurskov Nielsen, O.; Praestgaard, E.; Rasmussen, U.; Kolomiyets, T. M.; Voyiatzis, G. A.; Anastasiadis, S. H. *J. Mol. Struct.* **1999**, *479*, 271.
(15) Kirillov, S. A.; Voyiatzis, G. A.; Kolomiyets, T. M.; Anastasiadis, S. H. *Phys. Lett. A* **1999**, *262*, 186.
(16) Faurskov Nielsen, O. *Annu. Rep. Prog. Chem., Sect C, Phys. Chem.* **1993**, *90*, 3.

(17) Kirillov, S. A.; Yannopoulos, S. N. *Phys. Rev. B* **2000**, *61*, 11391.
(18) Novikov, V. N. *Phys. Rev. B* **1998**, *58*, 8367 and references therein.
(19) Winterling, G. *Phys. Rev. B* **1975**, *12*, 2432.
(20) Martin, A. J.; Brenig, W. *Phys. Status Solidi B* **1974**, *64*, 163.
(21) Malinovsky, V. K.; Sokolov, A. P. *Solid State Commun*. **1986**, *57*, 757.
(22) Kirillov, S. A. *J. Mol. Struct*. **1999**, *479*, 279.
(23) Theodorakopoulos, N.; Jäckle, J. *Phys. Rev. B* **1976**, *14*, 2637.
(24) Kirillov, S. A. *Chem. Phys. Lett*. **1999**, *303*, 37.
(25) Turrell, G. *Spectrosc. Eur*. **1997**, *9* (4), 8; *9* (6), 10.
(26) Kirillov, S. A. *J. Mol. Liq*. **1998**, *76*, 35.
(27) Kirillov, S. A.; Faurskov Nielsen, O. *J. Mol. Struct*. **2000**, *526*, 317.
(28) Fytas, G.; Kanetakis, J.; Momper, B.; Akcasu, A. Z. *J. Chem. Phys*. **1991**, *95*, 6866.
(29) Brodsky, M. H.; Lukovsky, G.; Chen, M. F.; Plaskett, T. S. *Phys. Rev. B* **1970**, *2*, 3303.
(30) Stephen, M. J. *Phys. Rev*. **1969**, *187*, 279.
(31) Leibler, L. *Macromolecules* **1980**, *13*, 1602.
(32) Fredrickson, G. H.; Helfand, E. *J. Chem. Phys*. **1987**, *87*, 697.
(33) Kittel, C. *Quantum Theory of Solids*; Wiley: New York, 1987; Chapter 19.